Modification of the edge transport barrier by resonance magnetic perturbations

V. Rozhansky[1], E. Kaveeva[1], P. Molchanov[1], I. Veselova[1], S. Voskoboynikov[1], D. Coster[2], A. Kirk[3], S. Lisgo[3], E. Nardon[3]

[1]St.Petersburg State Polytechnical University, Polytechnicheskaya 29, 195251 St.Petersburg, Russia

[2] Max-Planck Institut für Plasmaphysik, EURATOM Association, D-85748 Garching, Germany

[3]EURATOM/UKAEA Fusion Association, Culham Science Centre, Abingdon, Oxon, OX14 3DB, UK

E-Mail: rozhansky@edu.ioffe.ru

PACS numbers: 52.25.Fi, 52.55.Fa, 52.65.Kj

Abstract

The impact of resonance magnetic perturbations (RMP) on the structure of the edge transport barrier has been studied. A new model for the density pump-out mechanism during the stochastization of the plasma edge is proposed. The observed phenomena are explained as a result of the impact of the ambipolar electric field, which is modified during RMP, on the particle fluxes in the pedestal region. It is demonstrated that the rise of the particle fluxes inside the transport barrier leads to the pump-out effect on density, while the pedestal temperature increases in spite of the big electron heat conductivity in the stochastic magnetic field. The analytical approach is supported by results of simulations with the B2SOLPS5.2 2D transport code which uses a full description of particle sources and transport phenomena in the pedestal region. Simulations are performed for ASDEX Upgrade and MAST configurations for various values of electron stochastic conductivity. The radial electric field with RMPs is predicted to be less negative than without RMP. The density drop and temperature rise in the pedestal region are observed in accordance with the experimental results. Generation of toroidal rotation in the co-current direction is predicted. Extrapolations to ITER are discussed.

1. Introduction

It was demonstrated on DIII-D [1] and later on JET [2] that edge localized modes (ELMs) could be suppressed or mitigated by applying resonance magnetic perturbations (RMP) to the high confinement regime (H-regime) of a tokamak. The resonance coils for RMP are installed or planned on almost all large tokamaks: DIII-D, JET, MAST, ASDEX-Upgrade(AUG) and ITER. The widely accepted mechanism of ELMs suppression during RMP is reduction of the pressure gradient in the pedestal region below the stability limit for type I ELMs. The main contribution to the pressure gradient decrease is the pedestal density drop – the so-called 'pump-out effect', while the pedestal temperature does not drop and might even increase. Up to now this effect was not understood. At first glance during the formation of the ergodic magnetic layer which is created by RMP both density and electron temperature should decrease together since diffusion and electron heat conductivity coefficients should rise simultaneously. On the other hand, as was known from several earlier [3] and recent [4, 5, 6] observations, inside the stochastic layer the radial electric field becomes less negative or even positive and co-current toroidal rotation is generated. In the existing model [7] special assumptions for the transport coefficient were invoked to explain the observed phenomena. A neoclassical simulation [5] can reproduce the typical features observed in the experiment but in the present form the code does not contain pedestal sources and realistic turbulent transport coefficients nor does it include a mechanism for the generation of toroidal rotation.

In the present paper the observed phenomena are explained quite naturally as a result of the impact of the ambipolar electric field, which is modified during RMP, on the particle fluxes in the pedestal region. It is demonstrated that the rise of the particle fluxes inside the transport barrier leads to the pump-out effect on density, while pedestal temperature increases in spite of the big electron heat conductivity in the stochastic magnetic field. The analytic model is similar to that discussed recently in [8]. The analytic approach is supported by results of simulations with the B2SOLPS5.2 2D transport code with full treatment of particle sources and transport phenomena in the pedestal region. Simulation results are in agreement with the pump-out effect observed on MAST for H-mode provided the strong screening of vacuum magnetic perturbations takes place. A weak pump-out effect is predicted for L-mode, which is in qualitative agreement with DIII-D observations [9] but contrasts the MAST results. The strong pump-out effect for MAST might be interpreted as a rise of effective transport coefficients.

2. Analytic model

It is assumed that a stochastic layer is created with a width close to the width of the edge transport barrier (ETB). We are not considering here effects of plasma response to the vacuum magnetic perturbations, in particular, possible screening of the vacuum magnetic field [10], the self-consistent magnetic perturbations are treated as a given quantity. The radial current density of electrons in a stochastic magnetic field is given by a simple expression [11] (y is a dimensionless radial coordinate, h_y is the metric coefficient)

$$j_e = \sigma_{St}(E_y + \frac{T_e}{e}\frac{d\ln n}{h_y dy} + 0.5\frac{T_e}{e}\frac{d\ln T_e}{h_y dy}) . \qquad (1)$$

The coefficient 0.5 here corresponds to the collisionless limit. The stochastic conductivity is $\sigma_{St} = k(ne^2/T_e)\chi_e^{RR}$ with χ_e^{RR} being the Rechester-Rosenbluth expression for electron heat conductivity [12], and $k<1$ is a numerical coefficient. The electron current in a stochastic magnetic field is compensated by a neoclassical ion current j_i, which depends on the self-consistent radial electric field. The neoclassical ion current might be obtained from the balance of the average parallel classical viscous force, the divergence of the radial flow of parallel momentum and the ion-neutral friction force in the averaged parallel momentum equation, and from the balance of the divergence of the radial flow of toroidal momentum, ion-neutral friction and $\vec{j}_i \times \vec{B}$ force in the averaged toroidal momentum balance equation [13]-[14]

$$\langle\langle j_i \rangle\rangle = \sigma_{NEO}(E_y - E_y^{NEO}) , \qquad (2)$$

where the neoclassical electric field is (k_T is coefficient depending on collisionality [15], U_T is the toroidal velocity, $\langle\ \rangle$ and $\langle\langle\ \rangle\rangle$ correspond to volume and surface averaging).

$$E^{(NEO)} = \frac{T_i}{e}(\frac{1}{h_y}\frac{d\ln n}{dy} + k_T\frac{1}{h_y}\frac{d\ln T_i}{dy}) - \frac{B_p}{B}\langle BU_T \rangle . \qquad (3)$$

The neoclassical conductivity is $\sigma_{NEO} = 3\mu_{i1}B_p/2R^2B\langle BB_p \rangle$. The viscosity coefficient μ_{i1} is introduced in [15]. In the collisional limit it coincides with the Braginskii parallel viscosity coefficient $\eta_0 = 0.96nT_i/\nu_i$. The surface averaged currents should satisfy the ambipolarity condition.

$$\langle\langle j_e \rangle\rangle = -\langle\langle j_i \rangle\rangle . \qquad (4)$$

An equation for the toroidal rotation velocity in the absence of external applied torque reads

$$\langle\langle j_i \rangle\rangle = -\left\langle\left\langle \frac{1}{B_p}\frac{1}{h_z\sqrt{g}}\frac{\partial}{\partial y}\left[\frac{h_z\sqrt{g}}{h_y}\left(m_i \Gamma U_T + G^{add} - \frac{\eta}{h_y}\frac{\partial U_T}{\partial y}\right)\right] + m_i n \nu_{iN}(U_T - U_T^N)\right\rangle\right\rangle . \quad (5)$$

Here U_T is the toroidal velocity of ions, U_T^N is the toroidal velocity of neutrals, ν_{iN} is the ion-neutral collision frequency, $\Gamma = -D\partial n / h_y \partial y$ is the particle flux in the absence of RMP. The quantity h_z is the toroidal metric coefficient, $\sqrt{g} = h_x h_y h_z$ and $\eta \sim n m_i D$ is the turbulent perpendicular viscosity coefficient. The additional term G^{add} corresponds to additional transport of toroidal momentum due to additional ion fluxes in the presence of a stochastic layer. It also contains neoclassical effects. According to Eq. (5) the plasma is accelerated in the toroidal direction by a $\vec{j}_j \times \vec{B}$ force caused by the radial ion current. Note that the electron current does not produce toroidal torque since the electron current flows along the magnetic field lines. The Eqs. (1-5) determine the radial electric field and toroidal rotation velocity during RMP. This equation system has been invoked to interpret experiments on Tuman-3M [16].

The radial ion particle flux in the presence of RMP consists of two parts

$$\Gamma_i \equiv \Gamma + \Gamma^{st} = \Gamma + j_i / e . \quad (6)$$

The first term is a turbulent flux proportional to the density gradient while the second one is caused by the induced ion current. Note that according to the ambipolarity condition $\langle\langle \Gamma_e \equiv \Gamma - j_e / e \rangle\rangle = \langle\langle \Gamma_i \rangle\rangle$. In the experiment the flux Γ^{st} might be large enough and comparable with Γ.

For example, for typical parameters of an AUG H-mode [17]-[18], Figs.1-3, the Rechester-Rosenbluth heat conductivity can be estimated as $\chi_e^{RR} = D_{st}\sqrt{T_e / m_e} \sim 0.3 m^2 / s$ for the magnetic field perturbation in the plasma $B_r / B \approx 10^{-4}$, $D_{st} = 0.5 \cdot 10^{-7} m$, $T_e \approx 400 eV$. Here it is taken into account that according to modeling [19] the quasilinear approximation $D_{st} \approx 2\pi\, qR(B_r / B)^2$ for the diffusion coefficient of the magnetic field line gives value about 10 times larger than the real one. For $k = 0.3$, $n \approx 2 \cdot 10^{19} m^{-3}$, estimating radial derivatives as $(\partial / h_y \partial y)^{-1} \sim L \sim 1.5\ cm$ with L being the barrier width, we obtain an additional particle flux of ions $\Gamma^{st} = \sigma_{St} E / e \sim k\chi_e^{RR} n / L \sim 10^{20} s^{-1} \cdot m^{-2}$. This is of the order of the initial turbulent flux $\Gamma \sim Dn/L$ inside the barrier. For this estimate the neoclassical field Eq.(3) $E \sim T_i /(eL)$ is taken, $T_i \approx T_e$. The radial electric field is significantly reduced in absolute value $\left|E - E^{NEO}\right| \sim \left|E^{NEO}\right|$ due to stochasticity and therefore the additional ion flow can be overestimated. Indeed we calculated the ion flux using the initial electric field whereas it is necessary to use the self-consistent electric field. The modeling shows that for AUG parameters the stochastic ion flow is twice lower than that estimated due to the change of the radial electric field, Fig.4.

Inside the ETB the net flux is mainly determined by the particle sources in the barrier region. In the presence of Γ^{st} the turbulent particle flux Γ should be significantly reduced and hence the density gradient inside the barrier should drop considerably. To provide the same particle flux from the core as in the absence of RMP, the density gradient at the core side of the ETB should remain the same which leads to a considerable density drop at the pedestal, which corresponds to the 'pump-out' effect.

In contrast, the electron temperature gradient inside the ETB might not decrease at all. Here the rise of electron heat conductivity due to χ_e^{RR} is compensated by the decrease of the turbulent heat conductive flux (which is proportional to the density) due to the strong density drop. The rise of the convective electron heat flux due to Γ^{st} is compensated by the decrease of the diffusive flux. The final temperature profile depends on the interplay of the parameters. At the core side of the ETB, there is a density drop but no increase of the electron heat conductivity due to stochastisity. Here a more steep temperature profile is expected to provide the same energy flux and hence the electron temperature rise should take place.

3. Results of simulations with B2SOLPS5.2

The simulations were performed with the B2SOLPS5.2 code [18] adapted for H-mode modeling. In this code the system of fluid transport equations is solved including all perpendicular currents, ∇B drift, $\vec{E} \times \vec{B}$ drift, and drifts associated with viscosity. The equation system provides a transition to the neoclassical equations when the anomalous transport coefficients are replaced by the classical values. In order to account for the stochastization an additional radial electron current and additional electron heat flow were introduced. The radial current is taken in the form Eq.(1) where the stochastic conductivity $\sigma_{St} = \alpha n$ is proportional to the plasma density. The heat flow of electrons has a contribution from the convective electron flow along the stochastic field lines and from the additional heat conductivity caused by stochastization:

$$q_y^{stoch} = -\frac{5}{2} T_e \frac{j_e}{e} - \chi_e^{RR} \frac{nT_e}{e} \frac{\partial \ln T_e}{h_y \partial y} . \tag{7}$$

where $\chi_e^{RR} = k^{-1} \sigma_{St} T_e /(ne^2)$, $k = 0.3$. The standard source term $-\frac{j_e}{en} \frac{\partial n T_e}{h_y \partial y}$ was added to the r.h.s. of the electron heat balance equation.

For the modeling of ASDEX-Upgrade the geometry and pedestal parameters of shot №17151 [18] were taken. Several flux surfaces just inside the separatrix are chosen for the stochastic layer, the width of the layer at the outer mid-plane is 2 *cm*. The transport barrier width is 1.5 *cm*, so it is situated entirely inside the stochastic zone. The coefficient α for stochastic conductivity was $2.8 \cdot 10^{-23}$ siemens·m^2. This value corresponds to a rather modest heat conductivity $\chi_e^{RR} = 0.14 \div 0.35 m^2 / s$. Nevertheless the changes in the radial electric field and plasma profiles are large. In order to simulate the change in pedestal plasma density and temperatures the net particle flow, electron and ion heat flows from the core with and without stochastization were kept the same. The density profiles are shown in Fig. 1a, while the ion flows through flux surface as a function of radius are shown in Fig. 1b. Almost the same flow through the inner boundary and the same ionization sources in the barrier region (the latter is reflected by the increase of ion flow towards the separatrix) correspond to different pedestal densities with and without stochasticity. In the case of stochasticity the density at the inner boundary (in the core) is $n_e|_{core}=2.5 \cdot 10^{19}$ m^{-3}, while without stochasticity the density is $n_e|_{core}=4.3 \cdot 10^{19}$ m^{-3}. The pump-out effect is rather large.

The temperature profiles for electrons and ions are shown in Figs. 2-3. The electron and ion pedestal temperature rise due to stochasticity is 60*eV* and 160*eV*. The temperature rise is compensating the reduction of the turbulent radial heat conductive flow for smaller density. The Rechester-Rosenbluth electron heat flow cannot contribute significantly to the net energy flux balance since it is relatively small (stochastic heat flow is only 0.24 *MW* at the inner boundary of stochastic layer while the turbulent conductive heat flow of electrons is 0.72 *MW*). Note that the turbulent heat conductivity inside the barrier remains large, it is reduced only by a factor of 2 [17]-[18], therefore the turbulent heat flow inside the barrier is still twice bigger than the stochastic heat flow. The key role is the effect of the density decrease.

The radial electric field is shown in Fig. 4. More positive (less negative) electric field in the case of stochasticity corresponds to the positive ion current 350 *A*, which compensates the electron loss along the stochastic field lines. The decrease of the absolute value of radial electric field leads to smaller values of poloidal rotation shear, Fig.5, and so further ergodization might cause a H-L back transition.

The base calculations were made for a discharge with NBI, so the parallel velocity in the core was prescribed by the boundary conditions. In the calculations with the stochastic layer the toroidal momentum flow from the core was kept the same as in the base calculations, in order to trace the impact of the stochastic layer on the plasma rotation. The parallel velocity in the case of ergodization, Fig. 6, is more negative (negative sign corresponds to the co-current rotation) due to plasma spin-up by the ion radial current, Eq.(5). The terms on the r.h.s. of Eq.(5) for the AUG parameters are of the same order so that the increase of the parallel velocity can be estimated as $\Delta U_T \sim 0.25 j_e L^2 B_p / \eta \sim 2.5 \cdot 10^4 m/s$ which is of the same order as in the simulations, Fig. 6.

The choice of the stochastic conductivity dependence on plasma parameters is not so important for the mechanism of the pump-out effect provided the average value of conductivity is the same. The calculations with the constant stochastic conductivity $5 \cdot 10^{-4}$ *siemens/m* in the stochastic layer give results similar to those with the density dependent conductivity.

For MAST simulations the recent H and L-mode experiments with edge stochastization were chosen. The H-mode shot №20381 with stochastic coils off and the shot №20387 with stochastic coils on have very similar parameters except the current in the coils. The stochastic layer width was taken to be equal to the edge transport barrier width (2.4 *cm* at the outer mid-plane) and the constant stochastic conductivity was chosen. The best fit with experiment was reached for the value of the stochastic diffusion coefficient in the middle of the barrier equal to $D_{St} = 0.6 \cdot 10^{-7} m$. This value corresponds to stochastic conductivity $2.5 \cdot 10^{-3}$ *siemens/m* and stochastic electron heat conductivity $\chi_e^{RR} = 0.2 m^2/s$.

The vacuum diffusion coefficient of magnetic field lines was calculated using the ERGOS code [20], which can trace magnetic field lines. The value of the coefficient D_{FL} in a flux space was calculated using a deviation of the magnetic field line Δs from the initial flux surface after N toroidal turns: $D_{FL} = 0.5\left\langle (\Delta s)^2 \right\rangle / N$. Here $s = \sqrt{\Psi^n}$ is a function of the normalized poloidal flux $\Psi^n = \Psi / \Psi_s$, with Ψ_s being the poloidal flux at the separatrix.

For shot №20387 the coefficient is $D_{FL} = 0.5 \cdot 10^{-5}$. The local diffusion coefficient of the magnetic field lines in real space was calculated for the equatorial mid-plane using the expression

$$D_{St} = \frac{\Psi_s^2 D_{FL}}{B_p^2 (\pi R)^2 \left\langle L_{\|} \right\rangle}. \tag{8}$$

Here $\langle L_{\parallel} \rangle$ is the length of the magnetic field line divided by the number of toroidal turns. The diffusion coefficient calculated according to Eq. (8) is $D_{St} = 4 \cdot 10^{-7} m$, which is about 7 times bigger than the value chosen for simulations. This might be an indication of the strong screening of the vacuum magnetic field.

The experimental and simulated density profiles for H-mode MAST shots №20387 and №20381 are shown in Fig. 7. As for AUG the net particle flow, electron and ion heat flows from the core with and without stochastization were kept the same. The strong density drop in the pedestal region corresponding to the pump-out effect is observed both in the experiment and in the simulation. The calculated electron temperature profiles are almost the same with and without stochasticity, Fig. 8. The effect of the Rechester-Rosenbluth heat conduction turn on and that of the decrease of the turbulent heat transport with density compensate each other. In the experiment within the barrier the measured temperature is smaller with the stochasticity switched on while the electron temperatures at the core side of the barrier with and without stochasticity are the same. The radial electric field is shown in Fig. 9 and its shear in Fig.10. The shear decrease in the stochastic case is predicted as in the AUG case.

For the L-mode experiments the shot №20449 with stochastic coils off and shot №20451 with stochastic coils on were simulated. The experimental profiles, Fig. 11, reveal significant pump-out effect. The simulations with various values of stochastic conductivity were performed. Even for very large values of σ_{St} the calculated pump-out effect was very modest. The increase of the stochastic layer width also did not help. A small pump out effect is expected also from the analytical model since the neoclassical current is proportional to the density and temperature gradients and therefore should be small in the L-mode. A weak pump-out effect in the L-mode has been reported for DIII-D [9], while for MAST it was quite big. In order to match the experiment for MAST we were forced to increase the turbulent diffusivity in the case of the stochastic layer. The anomalous diffusion coefficient was chosen to be $D = 4.0 m^2/s$ without stochastization and $D = 7.7 m^2/s$ with stochastization. The simulated density profiles are shown in Fig. 11. This increase in turbulent transport is consistent in the increase in the density fluctuations measured by the reciprocating Langmuir probe. The physical reason for the increase of the turbulent transport in the L-mode with edge stochastization is unclear at present. The electron temperature profiles with and without stochastization are very similar as in the experiment.

4. Consequences for ITER

According to the model presented the level of the pump out effect and the level of radial electric field and its shear are determined by stochastic conductivity, by neoclassical conductivity and by the turbulent particle flux. For a given value of magnetic perturbations B_r / B the stochastic conductivity is proportional to $\sigma_{St} = k(ne^2 / T_e)\chi_e^{RR} \sim nqR / T_e^{1/2}$. This value should be larger for ITER than for AUG or MAST mainly due to the dependence on the major radius R. Note, however, that the neoclassical conductivity is $\sigma_{NEO} = 3\mu_{i1} B_p / 2R^2 B \langle BB_p \rangle$. For the same value of μ_{i1} it is proportional to $R^{-2}B^{-2}$. The value of μ_{i1} might be of the same order or smaller for ITER than, for example for AUG. Hence, due to the $R^{-2}B^{-2}$ dependence we might expect that the value of σ_{NEO} for ITER might be two orders of magnitude smaller than for AUG or MAST!

Hence, there are two consequences.

i. For ITER a stronger impact of RMP on the radial electric field might be expected. In particular, we shall have the situation with $\sigma_{St} >> \sigma_{NEO}$. This corresponds to the positive radial electric field in the stochastic region. This might have impact on the H-mode.

ii. The particle flux Γ^{St}, which is proportional to the ion current, is also reduced as $R^{-2}B^{-2}$ and for $\sigma_{St} >> \sigma_{NEO}$ its maximal value according to Eq. (2) does not exceed $\Gamma^{St} \sim n\chi^{NEO} / L$, where χ^{NEO} is a neoclassical ion heat conductivity. The pump out effect would depend on the ratio of χ^{NEO} and turbulent diffusion coefficient D inside the barrier. If D inside the edge barrier is of the order of $D \sim 0.1 m^2 / s$, which is typical for existing tokamaks, then the pump out effect for ITER will be very weak. On the other hand, if the turbulent diffusion coefficient will be also reduced with respect to existing tokamaks, due to, for example, a gyroBohm dependence, then the pump out effect might be considerable.

Conclusions

A new theoretical model for the density pump-out mechanism during the stochastization of the plasma edge is put forward. The density decrease is the result of a self consistent redistribution of radial plasma flows in the ambipolar electric field modified due to the electron loss along the stochastic field lines. The radial electric field is predicted to be more positive than without stochastization. The temperature increase in the pedestal region due to the density decrease is predicted. Plasma spin up due to the ion radial current in the co-current direction is expected. The model is in a good agreement with the results of simulation by the B2SOLPS5.2 code.

Simulation results are in agreement with experimental pump-out effect observed on MAST for H-mode provided the strong screening of the vacuum magnetic perturbations takes place. The weak pump-out effect is predicted for L-mode, which is in qualitative agreement with DIII-D observations but contrasts the MAST results. The strong pump-out effect for MAST might be interpreted as a rise of turbulent transport coefficients.

Figures

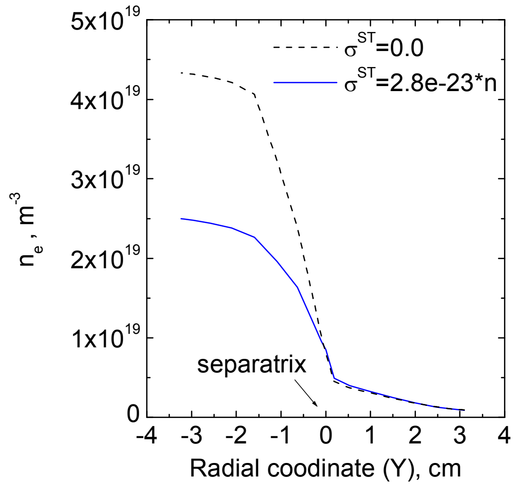

Fig. 1a. Electron density profile at the outer mid-plane with and without stochastic effects on AUG.

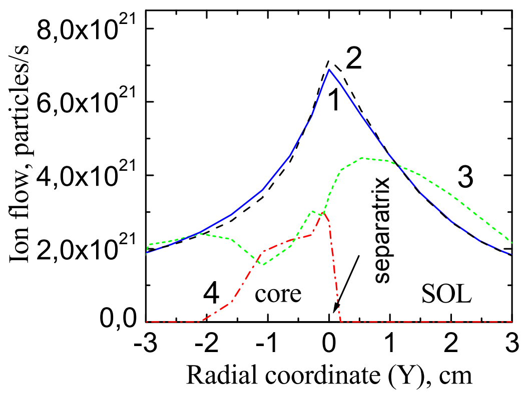

Fig.1b. Particle flows on AUG with and without stochastic layer. 1 – net flow through the flux surface with stochasticity; 2 –net flow without stochasticity; 3 – diffusive flow Γ with stochasticity; 4 – electron current-induced flow with stochasticity Γ^{st} .

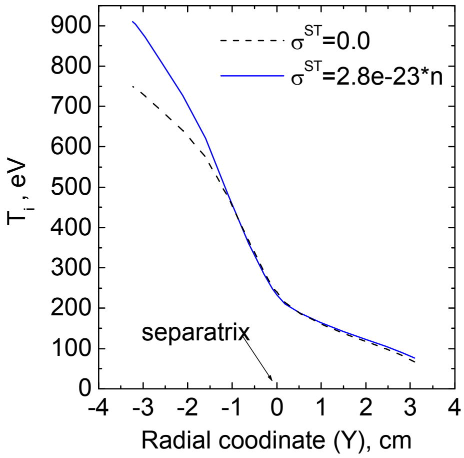

Fig. 2. Ion temperature profiles at the outer mid-plane with and without stochastic effects on AUG.

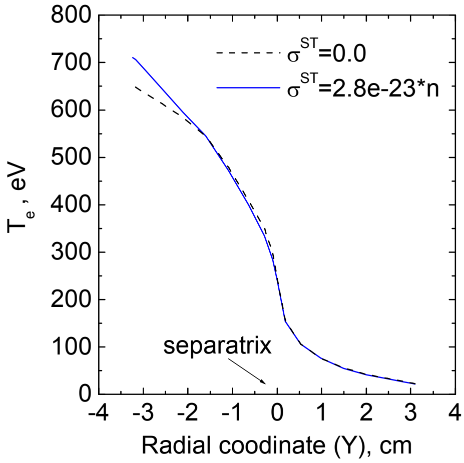

Fig. 3. Electron temperature profiles at the outer mid-plane with and without stochastic effects on AUG.

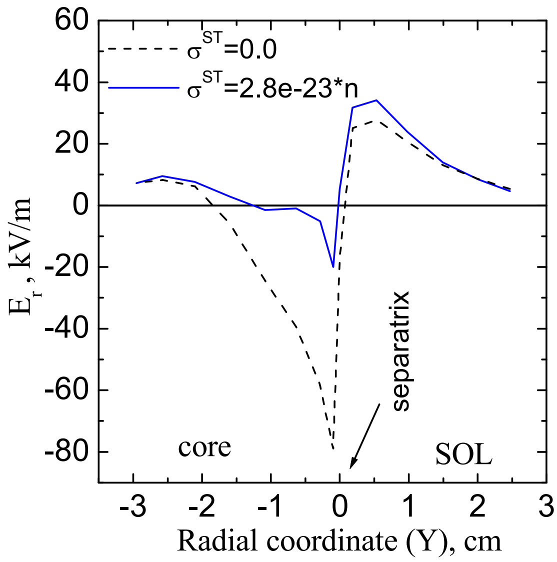

Fig. 4. Radial electric fields at the outer mid-plane with and without stochastic effects on AUG.

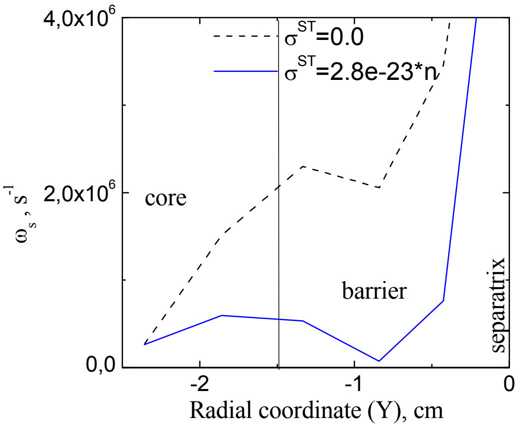

Fig. 5. Shear of poloidal rotation at the outer mid-plane with and without stochastic effects on AUG.

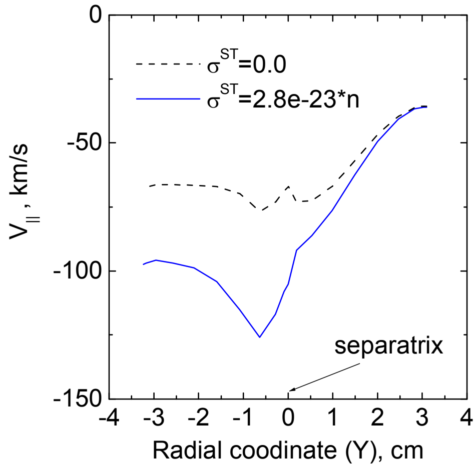

Fig. 6. Parallel velocity at the outer mid-plane with and without stochastic effects on AUG.

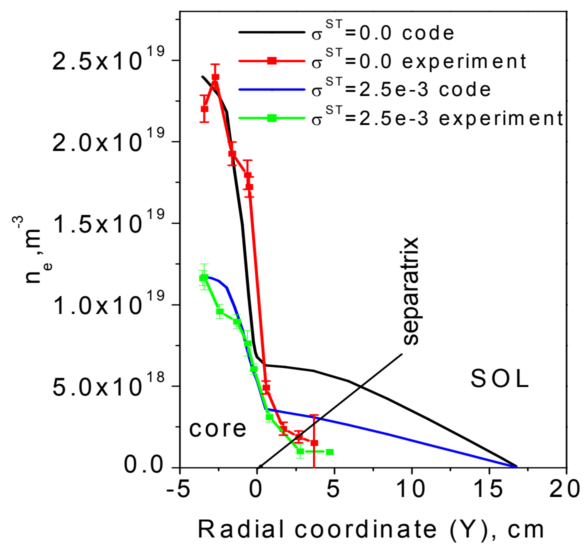

Fig.7. Electron density profile at the outer mid-plane with and without stochastic effects for H-mode shots on MAST.

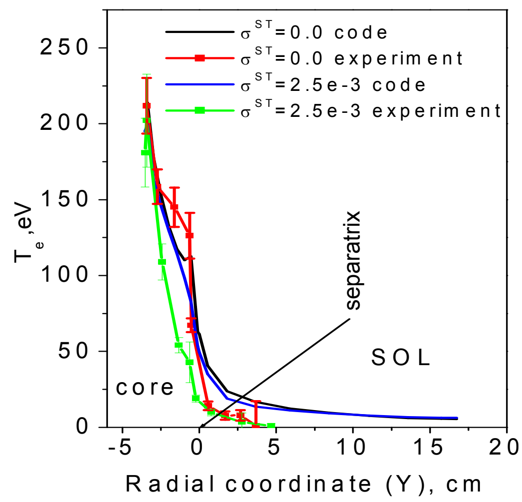

Fig.8. Electron temperature profiles at the outer mid-plane with and without stochastic effects for H-mode shots on MAST.

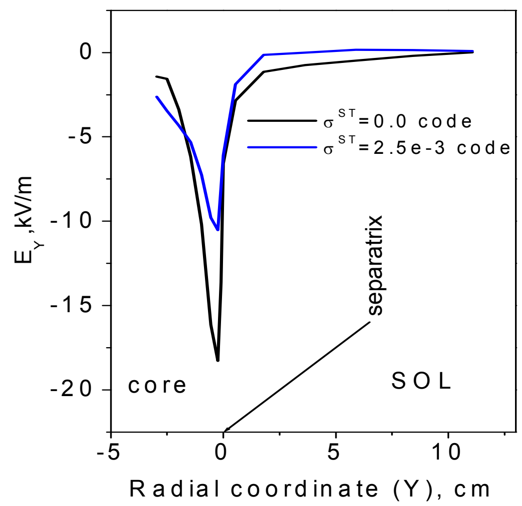

Fig.9. Radial electric fields at the outer mid-plane with and without stochastic effects for H-mode shots on MAST.

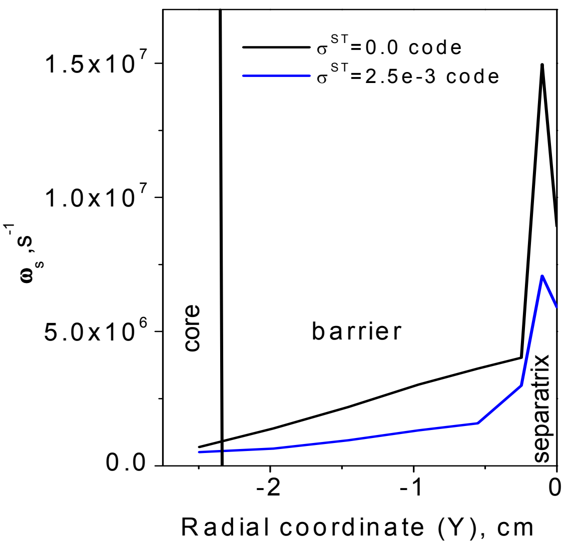

Fig. 10. Shear of poloidal rotation at the outer mid-plane with and without stochastic effects for H-mode shots on MAST.

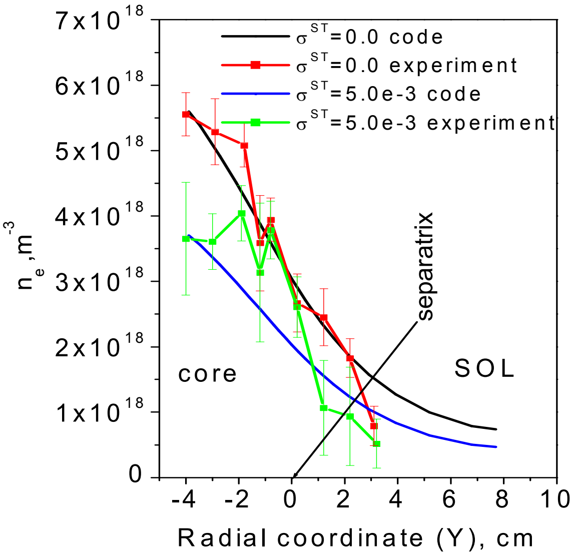

Fig. 11. Electron density profile at the outer mid-plane with and without stochastic effects for L-mode shots on MAST.

References

1. T.E. Evans *et al.,* Nucl. Fusion **48** 024002 (2008)
2. Y. Liang *et al*., Phys. Rew. Lett. **98** 265004 (2007)
3. X. Z. Yang *et al*., Phys. Fluids **B3** 3448 (1991)
4. B. Unterberg *et al*.**,** J. Nucl. Mater. **363** 698 (2007)
5. R. A. Moyer *et al*., J. Nucl. Mater. (2008) to be published
6. L. Askinazi *et al*, Plasma Phys. Contr. Fusion **48** A85 (2006)
7. M. Z. Tokar *et al*., Phys. Rev. Lett. **98** 095001 (2007)
8. M. Z. Tokar *et al*., Phys. Plasmas **15** 072515 (2008)
9. T. E. Evans, R. A. Moyer, P. Monat Phys. Plasmas **9** 4957 (2002)
10. R. Fitzpatrick, Phys. Plasmas 5 3325 (1998)
11. I. Kaganovich and V. Rozhansky, Phys. Plasmas **5** 3901 (1998)
12. A. B. Rechester and M. N. Rosenbluth, Phys. Rev. Lett. **40** 38 (1978)
13. V. Rozhansky *et al.,* Phys. Plasmas **9** 3385 (2002)
14. V. Rozhansky in Reviews of Plasma Physics **24** ed. by V.D. Shafranov, Springer (2008)
15. S.P. Hirshman and D.J. Sigmar, Nucl. Fusion **21** 1079 (1981)
16. E. Kaveeva *et al.,* Nucl. Fusion **48** 075003 (2008)
17. A.V. Chankin *et al.,* Plasma Phys. Control. Fusion **48** 839 (2006)
18. V. Rozhansky *et al.*, Nucl. Fusion **49** (2008) 025007
19. K. H. Finken *et al.*, Contrib. Plasma Phys. **46** 515 (2006)
20. E. Nardon *et al*., *J. Nucl. Mater.* **363-365** 107 (2007)